Virology 399 (2010) 299–311

Contents lists available at ScienceDirect

Virology

journal homepage: www.elsevier.com/locate/yviro

The role of Cajal bodies in the expression of late phase adenovirus proteins

Nicola J. James, Gareth J. Howell, John H. Walker, G. Eric Blair *

Institute of Molecular and Cellular Biology, Faculty of Biological Sciences, Garstang Building, Room 8.52d, Mount Preston Street, University of Leeds, Leeds LS2 9JT, UK

ARTICLE INFO

Article history:
Received 8 October 2009
Returned to author for revision
10 November 2009
Accepted 7 January 2010
Available online 4 February 2010

Keywords:
Adenovirus
Cajal bodies
Viral gene expression
Nuclear structure

ABSTRACT

Cajal bodies (CBs) are subnuclear structures involved in RNA metabolism. Here we show that, following infection of HeLa cells by adenovirus type 5 (Ad5), CBs fragment and form ordered structures, which we have termed "rosettes". Formation of CB rosettes was prevented by inhibition of viral DNA synthesis and preceded expression of the L4-33K protein. CB rosettes localised to the periphery of E2A-72K-containing replication centers and to the edges of ASF/SF2 and hnRNP A1 ring structures that demarcate sites of viral transcription and splicing. At later times of infection, CB rosettes were undetectable. Furthermore, knock-down of p80-coilin (the major structural protein of CBs) by RNA interference reduced the yield of infectious Ad5 and expression of the late proteins IIIa (from L1), hexon (from L3) and fiber (from L5), whereas the E2A-72K protein was unaffected. We conclude that CBs have an important role in the expression of adenovirus major late gene products.

Adenovirus infection of human cells subverts the normal nuclear processes of transcription and splicing to facilitate virus replication (Blair and James, 2005; Bridge and Pettersson, 1996; Bridge et al., 1995, Gama-Carvalho et al., 2003; Pombo et al., 1994; Reddy and Busch, 1998; Schul et al., 1996). While early viral gene expression does not alter the nuclear organisation of mRNA biogenesis, the onset of the late phase is accompanied by a marked redistribution of splicing factors (Bridge and Pettersson, 1996; Bridge et al., 1995). It has also been previously demonstrated that adenovirus infection leads to the fragmentation of Cajal bodies (CBs, also termed coiled bodies), although a functional significance has not been established (Rebelo et al., 1996; Rodrigues et al., 1996). CBs are highly conserved, intranuclear structures involved in RNA metabolism (Cajal, 1903; Cioce and Lamond, 2005). CBs typically number 1–10 per cell and range from 0.2 to 2 μm in diameter (Cioce and Lamond, 2005). Their size and number is determined by cellular stress, transcriptional activity and the level of splicing snRNPs (Carmo-Fonseca et al., 1993; Fernandez et al., 2002; Sleeman et al., 2001). CBs are capable of fusion and fission and can be either tethered to chromatin or are highly mobile (Dundr et al., 2004; Platani et al., 2000; Sleeman et al., 2003), associating with cleavage bodies, promyelocytic leukemic (PML) bodies and nucleoli (Cajal, 1903; Grande et al., 1996). It has been proposed that CBs are a heterogeneous group of related organelles with differing functions, reflected by variable composition (Alliegro and Alliegro, 1998; Sleeman and Lamond, 1999). Coilin is the major structural protein of CBs and is conventionally used as a marker (Andrade et al., 1993). Coilin knockout mice display reduced viability (Tucker et al., 2001). Coilin directly interacts with the survival of motor neurone (SMN) protein I component of splicing holoenzymes to recruit splicing snRNPs and is implicated in the pathology of spinal muscular atrophy (Herbert et al., 2001). CBs can be surrounded by transcription sites (Jordan et al., 1997), however since they lack nascent mRNA (Cmarko et al., 1999; Raska, 1995) and contain inactive RNA polymerase II (pol II) (Xie and Pombo, 2006), they have been proposed to be involved in assembly and regeneration of the transcription machinery rather than acting as sites of active transcription (Gall, 2000). CBs are enriched in spliceosomal snRNAs (Reddy and Busch, 1998) as well as components of the rRNA, mRNA and histone RNA processing pathways (Gall, 2000) and regulate the expression of U1 and U2 snRNAs (Smith et al., 1995).

Adenovirus-induced fragmentation of CBs has been reported to occur only in cells expressing the viral E2A-72K DNA binding protein (Rodrigues et al., 1996). The targeting of E2A-72K to discrete nuclear structures, comprising single-stranded DNA replication intermediates, coincides with the onset of viral replication and conventionally defines the transition to the late phase of infection (Puvion-Dutilleul and Puvion 1990a, 1990b). This transition is accompanied by fundamental changes in adenovirus gene expression. Early phase transcripts derived from the major late promoter are neither alternatively spliced nor elongated beyond the L3 polyadenylation sequence (Shaw and Ziff, 1980; Iwamoto et al., 1986). In contrast, in the late phase, the entire major late transcription unit (MLTU) is transcribed and alternative RNA splicing occurs to produce late viral transcripts. During the initial part of the late phase (which has been termed the intermediate phase), selective expression of L4-33K occurs facilitating the generation and translation of alternate transcripts that encode the late phase proteins involved in capsid structure and assembly (Farley et al., 2004; Larsson et al., 1992; Tormanen et al., 2006).

Abbreviations: Ad, Adenovirus; CB, AraC, cytosine arabinoside; Cajal, (or coiled) body; FFU, fluorescent focus-forming unit; moi, multiplicity of infection; siRNA, small interfering RNA; ssDNA, single-stranded DNA.

* Corresponding author. Fax: +44 113 3431407.
E-mail address: g.e.blair@leeds.ac.uk (G.E. Blair).

0042-6822/$ – see front matter © 2010 Elsevier Inc. All rights reserved.
doi:10.1016/j.virol.2010.01.013

We sought to further characterise the fragmentation of CBs and determine the timing of the fragmentation during the adenovirus life cycle relative to the onset of DNA replication, the formation of hnRNP A1 and ASF/SF2 ring structures and the selective expression of L4-33K. In addition we investigated a possible role for CBs in the progression of the viral late phase.

Results

CB rosettes form after the onset of viral DNA synthesis and prior to L4-33K expression

The structure and distribution of nuclear Cajal bodies (CBs) in uninfected HeLa cells was determined by immunofluorescent anti-body staining of the major CB structural component, coilin (Fig. 1A). HeLa cell nuclei typically contained between 2 and 4 CBs per nucleus (Fig. 1A, arrows), with an average of 3.4 ± 0.4 per cell (Fig. 1D). In order to determine CB size, CB diameters were measured at their maximum within optimal planes of focus. CBs in uninfected cells ranged from 0.7 to 1.1 μm in diameter with an average of 0.9 μm (Fig. 1E).

Ad5 infection caused a radical alteration of the distribution and structure of CBs (Fig. 1B). More numerous foci were observed (Fig. 1D, 73.2 ± 3.9) which were smaller in diameter (Fig. 1E, 0.4 μm ± 0.01) than CB foci in uninfected cells and were organised into ring-type structures, which we have termed "rosettes" (Fig. 1B, arrowheads). The rings were not always aligned to the plane of focus and hence not all the CB rosettes within one nucleus were evident in the images. In

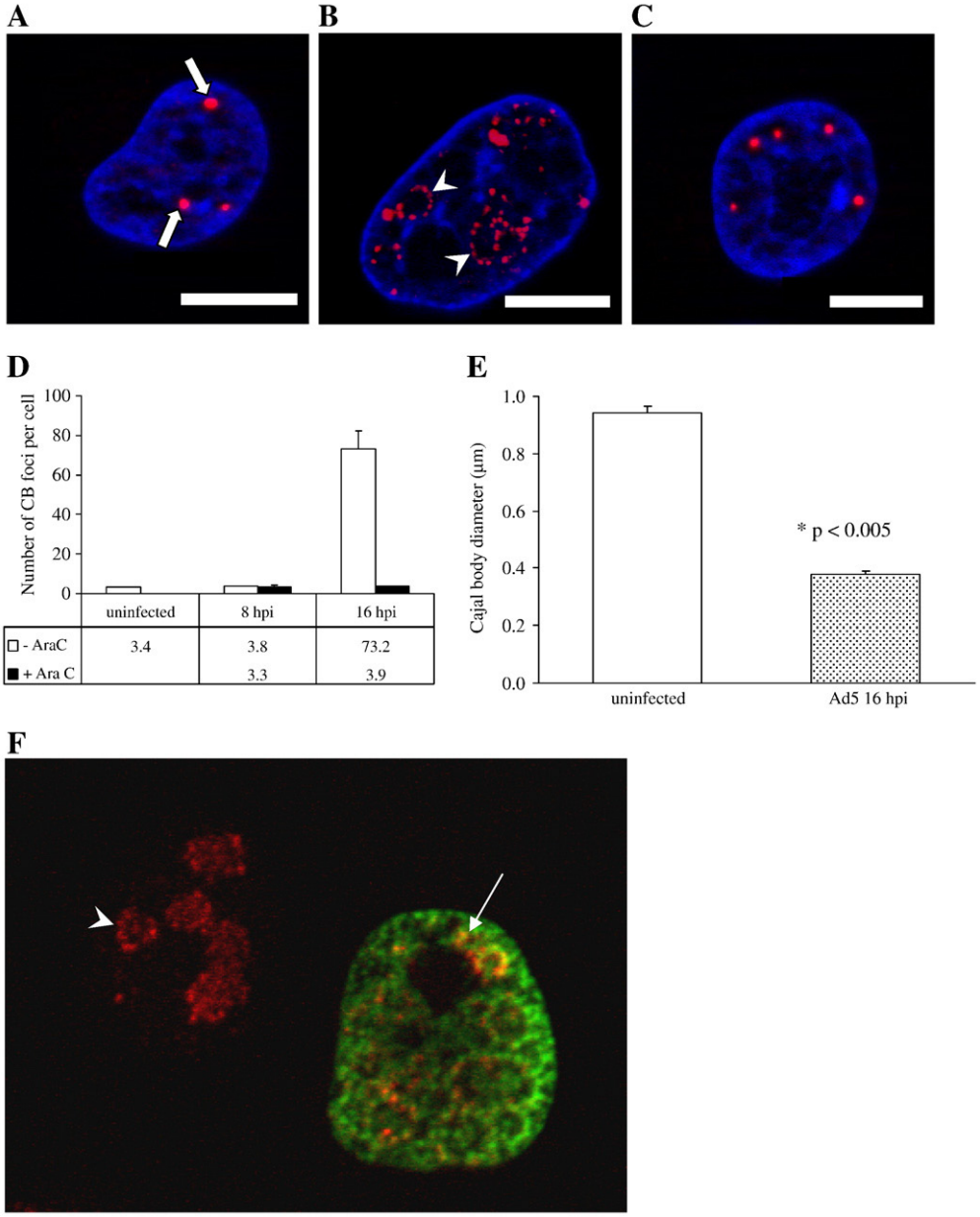

Fig. 1. Adenovirus-induced rearrangement of Cajal bodies occurs after the onset of DNA synthesis and prior to intermediate phase expression of the L4-33K protein. HeLa cells were infected with Ad5 (1000 FFU/cell) and fixed at 16 hpi. Coilin (red) was detected using rabbit anti-coilin followed by an AlexaFluor594-conjugated goat anti-rabbit secondary antibody. Nuclei were revealed using DAPI (blue). Cells were imaged in a single plane of focus by immunofluorescence microscopy. Images are representative of three independent experiments. (A) Arrows show CBs in uninfected cells. (B) Arrowheads show the reorganisation of CBs into rings of smaller foci ("rosettes") in infected cells. (C) CBs in Ad5-infected cells incubated in the presence of 25 μg/ml cytosine arabinoside, Ara C). (D) Ten random fields were scored for the number of large and small coilin foci (note that not all SEMs are visible). (E) The diameters of CBs in infected and uninfected cells were compared (Students' *t*-test, $p<0.005$). (F) Ad5-infected HeLa cells were permeabilised and incubated with mouse monoclonal anti-coilin (red) and rabbit anti-L4-33K (green). Arrowhead shows the appearance of CB rosettes prior to L4-33K expression. Cells positive for L4-33K showing CBs arranged as rosettes (arrow). Bar is equivalent to 10 μm.

addition, some CB foci were not part of a rosette structure. The average number of rosettes per field was 3.8 ± 0.9 and the average number of foci per rosette was 8.5 ± 1.2. In the presence of Ara C, which inhibits viral DNA replication (Gaynor et al., 1982), formation of CB rosette structures in Ad5-infected cells was prevented and the CBs were intact (Figs. 1C and D) suggesting that the formation of CB rosettes was dependent on viral DNA replication.

The onset of viral DNA replication marks the transition to the late phase of the adenovirus life cycle. The intermediate phase comprises the initial part of the late phase and is defined by the selective over-expression of mRNA from the L4 (L4-33K and L4-100K) and L1 (IIIa) regions of the MLTU (35). L4-33K expression enhances the selection of weak 3 splice sites of L1 transcripts, resulting in increased production of L1-IIIa at the expense of L1-52,55K (Farley et al., 2004; Larsson et al., 1992; Tormanen et al., 2006; Chow et al., 1979; Akusjarvi and Persson, 1981; Nevins and Wilson, 1981). L4-22K, whose sequence is related to L4-33K, also plays a role in the shift from the early to late phase (Morris and Leppard, 2009). In order to determine the temporal sequence of the formation of CB rosettes with respect to the ordered program of the expression of viral genes of the late phase, the expression of L4-33K and coilin staining was analysed by dual immunofluorescence microscopy (Fig. 1F). Fifty cells positive for L4-33K were examined for CB rearrangement and fifty cells displaying CB rearrangement were scored for L4-33K expression. Fig. 1F shows three typical cells within the same field. The two cells on the right show CB rosette formation characteristic of late phase viral infection. Cells staining positive for L4-33K (green) always contained CB rosettes (red), (Fig. 1F, cell to the right, arrow). However, CB rosette formation was seen in the absence of detectable L4-33K expression (Fig. 1F, cell to the left, arrowhead) but not *vice versa*, indicating that CB rearrangement occurs prior to L4-33K expression and thus prior to the onset of the intermediate phase of the virus life cycle. Since we have also shown that the rearrangement of CBs did not occur when viral DNA synthesis was inhibited (Figs. 1C and D), taken together, these results show that the formation of CB rosettes occurs at a precise time within the ordered sequence of events in the late phase of the viral life cycle, between the onset of DNA synthesis and the induction of L4-33K expression.

CB rosettes localise to the periphery of E2A-72K domains after the onset of viral DNA synthesis and are distinct from replication foci

Viral DNA replication is conventionally used to define the onset of the viral late phase. The accumulation of E2A-72K into spot, ring and crescent-like structures can be used as a marker for the onset of the late phase since these structures demarcate areas of active viral DNA replication (Pombo et al., 1994; Puvion-Dutilleul and Puvion, 1990a, 1990b, 1992). The latter two structures have previously been described as representing hollow spheres and open ended-goblets in three dimensions (Pombo et al., 1994). The domains labelled by anti-E2A-72K antibodies ("replication centers") contain single-stranded DNAs (ssDNAs) that are displaced from replication foci during the initial steps of viral DNA replication (Fig. 2A). Viral transcription sites and replication foci localise to the periphery of the E2A-72K-labelled ssDNA domains, although some replication foci may also be dispersed in the nucleoplasm (Pombo et al., 1994). Areas of active transcription are adjacent to replication foci but extend further from the E2A-72K centers into the surrounding nucleoplasm.

The spatiotemporal changes in CB distribution relative to immuno-reactive E2A-72K were determined in 100 cells at four-hourly intervals up to 20 h post-infection (hpi). The variety of E2A-72K and CB staining patterns observed were classified into different types (Figs. 2B–E). In order to facilitate comparison between the experimental results shown in Figs. 2, 3 and 4, type C acts as a temporal reference point and marks the appearance of coiled body rosettes. The data was used to determine the relative order of the changes in E2A-72K and CB patterns. A summary of the types of E2A-72K and coilin arrangements and the percentage contribution of each type to the total population at each time point is shown in Fig. 2F. In uninfected cells and in Ad5-infected cells up to 8 hpi, viral E2A-72K expression was not detected, while the CB pattern remained identical to that in uninfected cells. These cells were designated as type A (Fig. 2B). Cells consistently remained of the type A class until 8 hpi, when 20% of the cell population expressed E2A-72K homogeneously throughout the nucleus, but not within nucleoli, and the coilin distribution remained as in uninfected cells forming a second category of type A, termed type A1 (Fig. 2C). Differences in the intensity of E2A-72K expression were apparent between individual type A1 cells, indicating that viral infection progressed asynchronously, in agreement with previous observations (Gama-Carvalho et al., 2003). At 12 hpi, 57% of the population defined a new class, designated type B (Fig. 2D), where E2A-72K was present as spots (arrows) and rings (arrowheads) indicating the onset of viral DNA synthesis (Pombo et al., 1994; Puvion-Dutilleul and Puvion, 1990a, 1990b) while coilin remained distributed as in uninfected cells. Types A and A1 represented 21% and 22%, respectively, of the total population at this time point (Fig. 2F). We also noted that DAPI staining was more intense at the boundaries of the E2A-72K spots and rings (not shown). This is consistent with the accumulation of viral dsDNA at the boundaries of the ssDNA centers (Pombo et al., 1994). After 16 h of infection a new pattern was evident in 15% of the cell population, where coilin foci were observed to surround the periphery of spots and rings of E2A-72K (type C, Fig. 2E, arrows). It was evident that CB foci did not surround larger pools of E2A-72K (Fig. 2E, arrowheads), which correspond to increased levels of viral RNA synthesis (Pombo et al., 1994). Since the accumulation of DBP as spots and rings indicates active viral DNA synthesis, these results further support the proposal that CB rosette formation occurs after the onset of DNA synthesis, following from our previous observation that rosette formation was inhibited in the presence of Ara C.

Analysis of 50 cells showed that where CB rosette formation had occurred, E2A-72K was always present as accumulations of spots and rings. However, spots and rings of E2A-72K could be seen in cells where the CB pattern was of the uninfected cell type, showing that the fragmentation of CB into rosettes occurred after the accumulation of E2A-72K as spots and rings. Furthermore, the homogeneous expression of E2A-72K throughout the nucleus as seen in type A1 (Fig. 2C) was unaffected by inhibition of viral DNA synthesis with Ara C, whereas the formation of E2A-72K spots and rings was prevented by Ara C (data not shown). This is in agreement with the previous data showing that discrete centers of E2A-72K comprise active viral DNA replication sites (Pombo et al., 1994; Puvion-Dutilleul and Puvion, 1990a, 1990b, 1992).

It has been previously demonstrated that viral replication foci localise to the periphery of E2A-72K-labelled ssDNA domains (Pombo et al., 1994). We therefore determined whether the foci of CB rosettes and replication foci were coincident or separate. Replication sites were pulse-labelled with BrdU and detected using rat anti-BrdU followed by a FITC-conjugated goat anti-rat antibody. CBs were labelled with rabbit anti-coilin followed by an AlexaFluor594-conjugated goat anti-rabbit antibody. Examination of cells by fluorescence microscopy demonstrated that CB foci (red) were distinct from viral replication foci (green) (Fig. 2G).

ASF/SF2 ring formation precedes the appearance of CB rosettes

An extensive body of evidence suggests that splicing and transcription are spatially coupled (Aspegren and Bridge, 2002; Bentley, 1999; Beyer and Osheim, 1988; Neugebauer and Roth, 1997; Zeng et al., 1997). In adenovirus infection, it has been demonstrated that a proportion of pre-mRNA splicing occurs co-transcriptionally, although some splicing may also occur post-transcriptionally (Nevins and Darnell, 1978; Bauren and Wieslander,

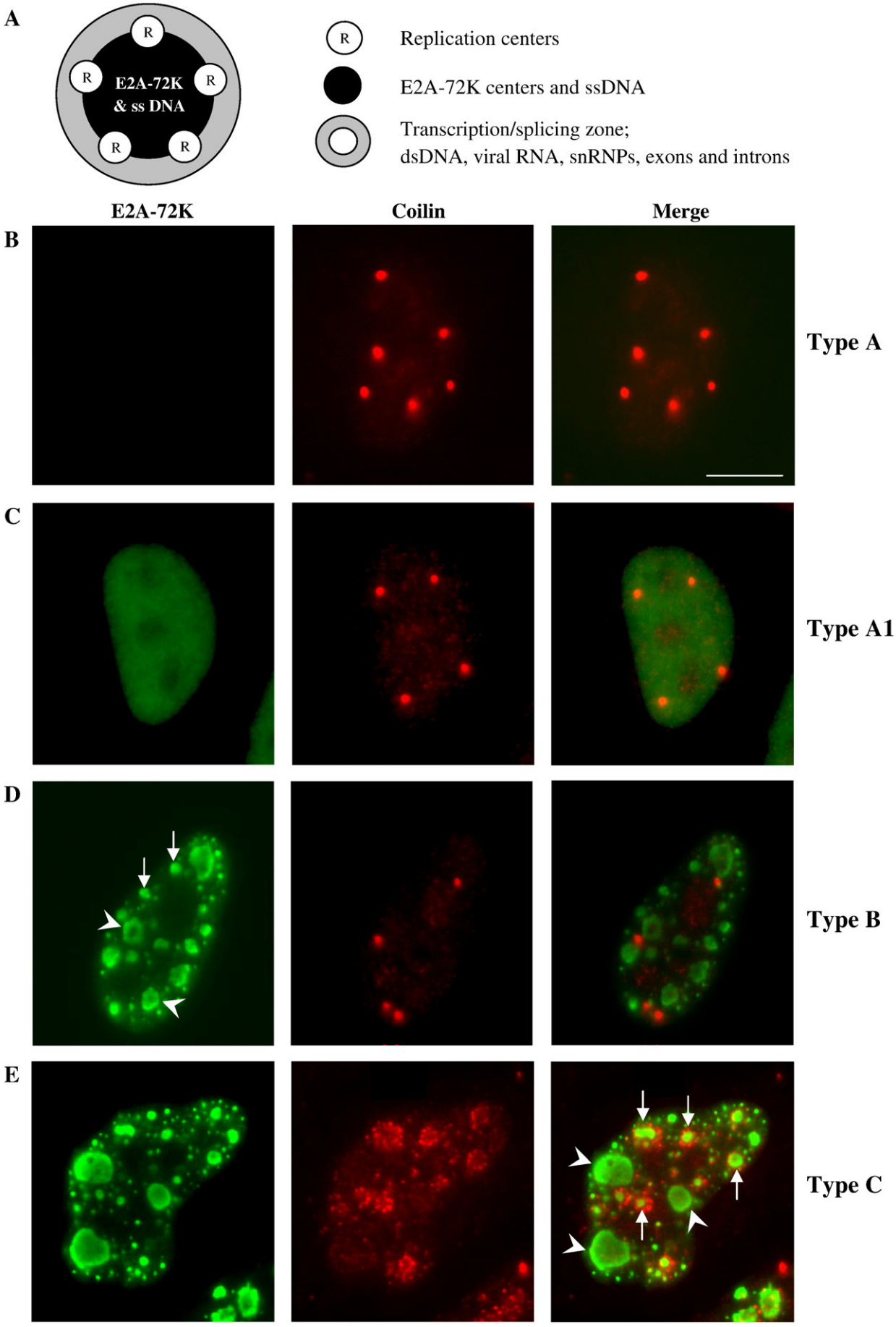
A
R
R
R
R
R
E2A-72K
& ss DNA
R
Replication centers
E2A-72K centers and ssDNA
Transcription/splicing zone;
dsDNA, viral RNA, snRNPs, exons and introns
E2A-72K
Coilin
Merge
B
Type A
C
Type A1
D
Type B
E
Type C

F

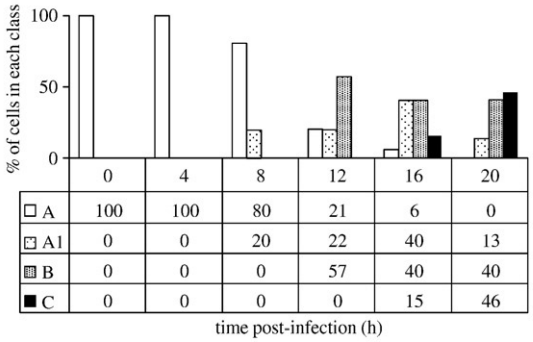

Type	CB Pattern	E2A-72K pattern
A	Uninfected	Not present
A1	Uninfected	Homogeneous
B	Uninfected	Spots & rings
C	Rosettes	Spots & rings

G

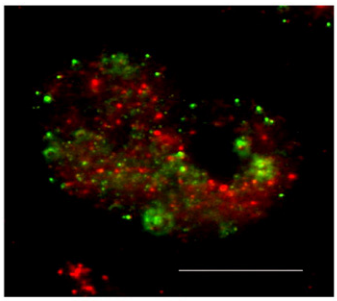

Fig. 2. Localisation of CB rosettes relative to sites of E2A-72K-containing structures and replication foci. (A) Schematic diagram of nuclear organisation of replication, transcription and splicing zones in Ad5-infected HeLa cells. (B–F) HeLa cells were infected with Ad5 (1000 FFU/cell) and harvested at four-hourly intervals up to 20 h. Cells were fixed, permeabilised and stained with rabbit anti-coilin followed by AlexaFluor594-conjugated goat anti-rabbit antibodies (red) then mouse anti-E2A-72K followed by AlexaFluor488-conjugated goat anti-mouse antibodies (green) and 100 cells were examined by immunofluorescence microscopy. Images of the staining patterns observed at 4, 8, 12 and 16 hpi are shown in panels B to E, respectively. Arrows designate E2A-72K-containing spots and arrowheads show E2A-72K-containing ring structures. (E) Arrows show the foci of CB rosettes localising to the periphery of E2A-72K spots. Arrowheads show the absence of CB rosettes at the periphery of enlarged E2A-72K pools. (F) A time-frequency distribution of the different staining types and a table of the characteristics of each coilin: DBP pattern type. "Uninfected," refers to CBs with the same pattern as in uninfected cells. (G) HeLa cells were infected with Ad5 (1000 FFU/cell). At 24 hpi, cells were pulse-labelled with 25 μM BrdU for 60 min. Labelled cells were fixed and permeabilised with 0.5% Triton X-100, prior to incubation with DNase II for 30 min. Replication foci were detected using rat anti-BrdU and AlexaFluor488-labelled goat anti-rat (green) antibodies. Coilin was detected using rabbit anti-coilin and AlexFluor594 conjugated goat anti-rabbit antibodies (red). Bar is equivalent to 10 μm.

1994; Nevins, 1983), especially of 3′ proximal introns. Splicing snRNPs locate to sites of transcription that surround sites of ssDNA accumulation, appearing as a series of inter-connected rings. Cells in this phase of viral infection have been designated as "ring cells" and this distribution of snRNPs is indicative of active transcription and splicing (Gama-Carvalho et al., 2003; Aspegren et al., 1998). We have demonstrated that CB rosettes localise to the periphery of ssDNA sites. The ssDNA domains are also surrounded by viral transcription and splicing sites, which extend further into the nucleoplasm than replication foci (Pombo et al., 1994; Puvion-Dutilleul and Puvion, 1990a, 1990b, 1992; Fig. 2A). We therefore investigated the localisation of CB rosettes relative to zones of active transcription and splicing, indicated by the organisation of ASF/SF2 into ring structures. Populations of 100 cells were examined at four-hourly intervals up to 20 hpi. The varieties of ASF/SF2 and coilin staining patterns observed were classified. These data were used to determine the relative order of changes in the patterns of CBs and ASF/SF2. Observation of the spatiotemporal changes in ASF/SF2 relative to coilin revealed that four different types of expression pattern were evident at different times up to 20 hpi (Figs. 3A–E). In uninfected cells and Ad5-infected cells up to 12 hpi, a single type of ASF/SF2 and coilin staining pattern was evident, where ASF/SF2 was apparent as speckled foci distributed throughout the nucleus (type A, Fig. 3A). ASF/SF2 speckles could also be seen within nucleoli (data not shown). At 16 hpi, around one fifth of the cells (21%) showed formation of inter-connected rings of ASF/SF2 (Fig. 3B, arrows) while the CB structure and distribution remained as in uninfected cells. Approximately two fifths (41%) of the cell population displayed rearrangement of CBs in conjunction with the ASF/SF2 ring structures (type C, Fig. 3C). CB foci that were arranged in rosette structures localised to the internal edges of the inter-connecting ring structures (Fig. 3C, arrows). ASF/SF2 ring structures contain nascent RNA as well as spliced exons derived from the tripartite leader sequence and introns (Rebelo et al., 1996; Aspegren and Bridge, 2002; Aspegren et al., 1998), thus the localisation of CB rosettes to the internal edges of the ASF/SF2 ring structures coincides with active transcription and splicing. After a further 4 h of infection, a novel type of staining was evident in which the rings of ASF/SF2 had disappeared, the levels of ASF/SF2 were reduced and spots of ASF/SF2 were evident. In addition, clusters of ASF/SF2, indicative of active viral mRNA export (Aspegren et al., 1998), localised to the nuclear periphery (Fig. 3D, arrows). At this stage of infection, some CB rosettes appeared to be in the process of disassembling as shown in Fig. 3D (type D, arrowheads). In addition, fifty cells displaying CB rosette formation were examined for the presence and pattern of ASF/SF2. All cells containing CB rosette structures also contained ring structures of ASF/SF2. In contrast, not every cell containing ASF/SF2 ring structures exhibited formation of CB rosettes, suggesting that the fragmentation of CB occurs after the formation of ASF/SF2 ring structures.

hnRNP A1 ring formation precedes the appearance of CB rosettes

Heterogeneous nuclear ribonucleoproteins (hnRNPs) bind nascent RNA, and some hnRNPs are implicated in the splicing reaction (Smith

and Valcarcel, 2000). hnRNP A1 antagonises the effect of splice site selection by ASF/SF2 (Bai et al., 1999). Both SR splicing factors and hnRNP A1 remain associated with the RNA after splicing is complete and are involved in the export of processed mRNA to the cytoplasm through nuclear pore complexes (Visa et al., 1996a, 1996b; Alzhanova-Ericsson et al., 1996). Anti-hnRNP A1 antibodies were used to determine CB localisation relative to RNA export and transcription/splicing zones. Populations of 100 Ad5-infected cells were analysed at

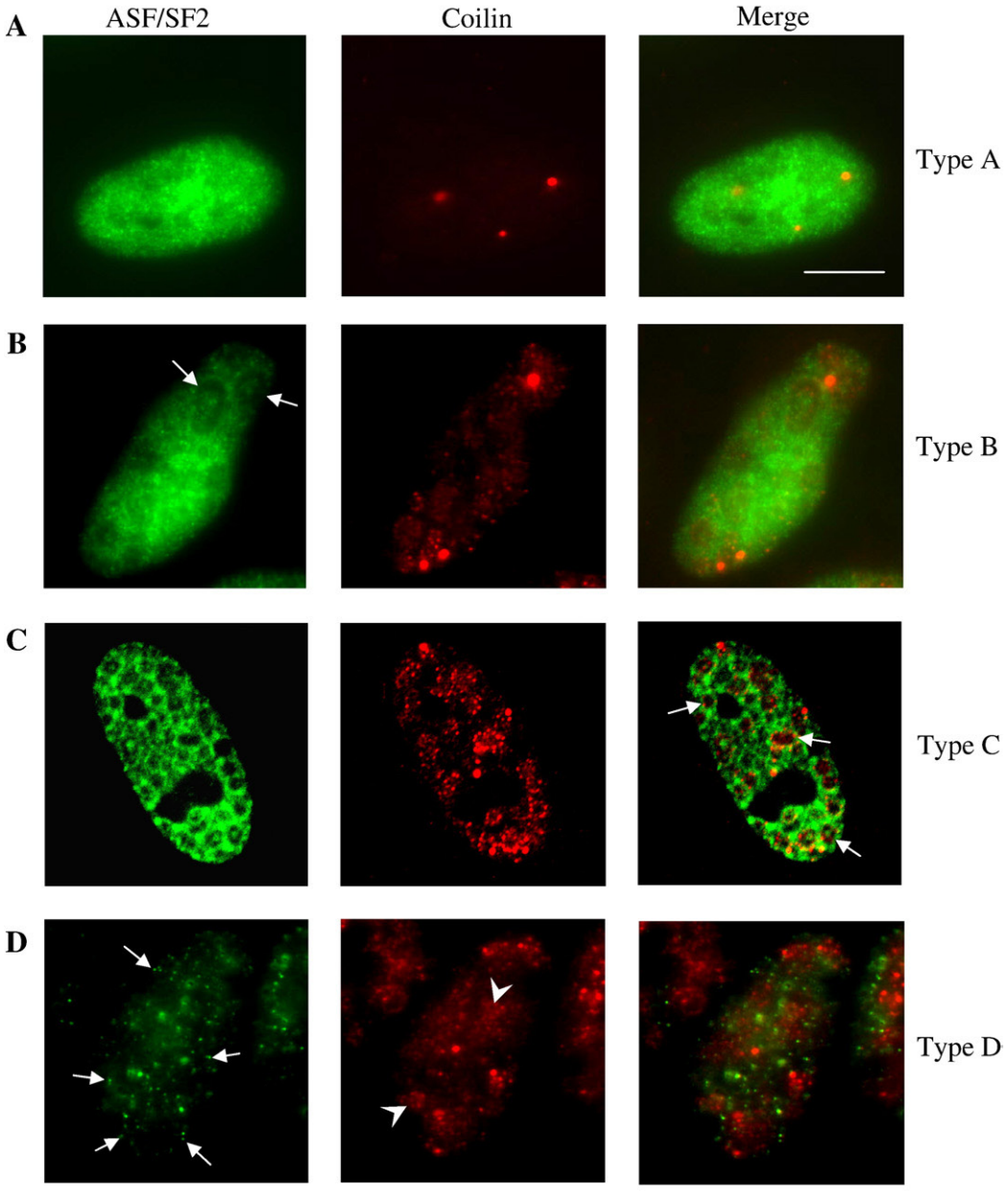

	0	4	8	12	16	20
A	100	100	100	100	38	34
B	0	0	0	0	21	0
C	0	0	0	0	41	0
D	0	0	0	0	0	66

Type	CB pattern	ASF/SF2 pattern
A	Uninfected	Speckles
B	Uninfected	Rings
C	Rosettes	Rings
D	Clusters	Clusters

four-hourly intervals up to 20 hpi. Different types of hnRNP A1: coilin staining were classified into a total of four distinct classes (Fig. 4A–E). Up to 8 hpi, a single hnRNP A1:coilin pattern type was observed (type A, Fig. 4A), where the hnRNP A1 was distributed as speckles evenly across the nucleus and CBs appeared as in uninfected cells. At 12 hpi, two new types of expression pattern, B and C, were evident. Type B (Fig. 4B) represented 29% of the total population, where the CBs remained as in uninfected cells (Fig. 1B, arrow) while hnRNP A1 was re-organised into a series of inter-connected rings (Fig. 4B, arrows), similar to the ring structures formed by ASF/SF2 (Fig. 3C). Type C (11%) was identical to type B in terms of the organisation of hnRNP A1, however CBs had fragmented and rearranged into rosette structures that aligned to internal edges of the hnRNP A1 ring structures (Fig. 4C, arrows). The onset of CB rosette formation occurred earlier (11% at 12 hpi) in comparison to their appearance at 16 hpi for the data shown in Fig. 2 (15% at 16 hpi) and Fig. 3 (41% at 16 hpi). These differences may be due to the asynchrony of viral infection, which has been observed previously (Gama-Carvalho et al., 2003), in combination with variation arising from sampling. Examination of 50 individual cells for the presence of hnRNP A1 rings and/or CB rosettes showed that the rearrangement of hnRNP A1 preceded the formation of CB rosette structures, since the formation of rosettes was not observed in the absence of hnRNP A1 ring structures but hnRNP A1 ring structures could be seen in the absence of CB rosette structures. At 16 hpi, a fourth type of hnRNP A1:coilin patterning (type D, Fig. 4D) was evident in 38% of the cell population. In type D cells hnRNP A1 was diminished and distributed as spots within the nucleus. Some of the hnRNP foci localised to the nuclear periphery (Fig. 4D, arrowheads), indicative of active export of viral mRNA (Visa et al., 1996a, 1996b; Alzhanova-Ericsson et al., 1996). CB rosettes were less well-defined (Fig. 4D, arrows), suggesting that some CB rosette structures had disassembled during the phase of enhanced viral mRNA export.

Taken together, the data shown in Figs. 2–4 indicate that CB rosettes form and localise to the periphery of the viral E2A-72K centers (an area of active transcription and splicing), during a short time period that occurs immediately after the onset of DNA synthesis, ASF/SF2 and hnRNP A1 ring formation and active transcription of late genes but prior to the onset of selective over-expression of L4-33K that characterises the onset of the intermediate phase (Larsson et al., 1992). Furthermore CB rosette structures disappear upon activation of enhanced viral mRNA export which is characterised by the formation of spots of ASF/SF2 and hnRNP A1 that accumulate at the nuclear periphery.

CBs are required for efficient expression of adenovirus late phase proteins

The potential involvement of CBs in the expression of late phase proteins was determined by depleting cells of coilin using siRNA. Western blotting and densitometric analysis showed that coilin protein levels were reduced by approximately 80% following knock-down with coilin-specific siRNA (Fig. 5A). The expression of three late phase proteins (L1-IIIa, L3-hexon and L5-fiber) was assayed using a flow cytometric method (Bottley et al., 2007). Expression of E2A-72K, which is expressed in both the early and late phases, was quantified in parallel as a control. Flow cytometry histogram analysis showed that the distributions of fluorescence intensities were bimodal for all the viral proteins assayed (Fig. 5B). The siRNA-mediated reduction of coilin expression resulted in 25–30% inhibition of the expression of the late phase proteins IIIa (L1), hexon (L3) and fiber (L5), which are translated from alternatively-spliced transcripts (Fig. 5C). In contrast, expression of E2A-72K was unaffected by coilin knock-down (Fig. 5C). These results revealed that knock-down of coilin expression reduced the production of late phase capsid proteins, without affecting expression of the E2A-72K protein.

Since adenovirus proteins are produced in excess and a substantial proportion are not assembled into infectious progeny (Green and Daesch, 1961), the effect of reduced coilin expression on production of infectious virus was determined using a virus yield assay. Cells infected with Ad5 following control or coilin siRNA treatment were harvested and lysates used to infect HeLa cells. Virus yield was determined by assaying the cells for hexon expression at 20 hpi. Reduction of coilin expression decreased virus yield by $30 \pm 2\%$ (a mean reduction $\pm$ SEM of three independent biological repeat experiments).

Coilin knock-down has no significant effect on distribution of Sp100 or fibrillarin in Ad5-infected HeLa cells

To determine the potential effect of coilin knock-down upon Ad5-induced reorganisation of other nuclear bodies (Blair and James, 2005; Weitzman and Ornelles, 2005), we investigated whether knock-down of coilin altered the pattern of changes in PML bodies, assessed by immunofluorescent antibody staining for Sp100 (Müller and Dejean, 1999) and nucleoli, assessed using fibrillarin localisation (Puvion-Dutilleul and Christensen, 1993). Examination of mock-infected HeLa cells showed that anti-Sp100 antibodies bound to spherical promyelocytic (PML) bodies in the nucleus (Supplementary Figure 2A). Ad5 infection of HeLa cells caused the PML bodies to fragment into smaller, more numerous speckles distributed throughout the nucleus (Supplementary Figure 2B). Knock-down using control or coilin siRNA had no significant effect upon the redistribution of PML induced by Ad5 infection (Supplementary Figure 2C and D respectively).

Examination of mock-infected HeLa cells showed that anti-fibrillarin antibodies bound to granule-like structures (Supplementary Figure 2E). Co-staining of fibrillarin and DNA (using DAPI) showed that fibrillarin was predominantly located within nucleoli in mock-infected HeLa cells (results not shown). Infection of HeLa cells with Ad5 caused the fibrillarin to form smaller foci, some of which co-localised with CB rosettes (Supplementary Figure 2F, arrows). The co-localisation of fibrillarin with CB rosettes seen in Ad5-infected cells was unaffected by treatment with control or coilin siRNA (Supplementary Figure G and H respectively). We conclude that knock-down using control or coilin siRNA had no significant effect upon the redistribution of fibrillarin induced by Ad5 infection.

Discussion

Ad5 infection of HeLa cells causes CBs to fragment into smaller foci (Rebelo et al., 1996; Rodrigues et al., 1996). Here, we show that these fragmented CB foci can form into organised structures and, when viewed along certain planes, appear as foci arranged in rings that we have termed “rosettes” (Fig. 1B). We have previously demonstrated that Ad5 infection alters the actin content of CBs (Gedge et al., 2005). Interestingly, the assembly of transcription complexes is dependent upon actin (Bettinger et al., 2004). The mechanism of CB rosette formation may thus be related to the actin content of CB, but requires further investigation.

The foci of the CB rosettes localised to the periphery of E2A-72K-containing spots and rings (Fig. 6A). The CB foci localised to the

Fig. 3. Spatiotemporal changes in the distribution of coilin relative to ASF/SF2. HeLa cells were infected with Ad5 (1000 FFU/cell) and harvested at 4-h intervals up to 20 hpi. Cells were fixed, permeabilised and stained with rabbit anti-coilin and AlexaFluor594-conjugated goat anti-rabbit antibodies (red) followed by mouse anti-ASF/SF2 and AlexaFluor488-conjugated goat anti-mouse antibodies (green). 100 cells were examined by fluorescence microscopy. Images of the staining patterns observed are shown in panels A to D. (B) Arrows show ASF/SF2 distribution in ring-like structures. (C) Arrows indicate CB rosettes localised to the periphery of ASF/SF2 ring structures. (D) ASF/SF2 spots at the nuclear periphery (arrows) and CB rosettes disassembling (arrowheads), 20 hpi. (E) A time–frequency distribution graph of the different staining patterns and a table of the characteristics of each coilin/ASF/SF2 pattern type. “Uninfected”, refers to CBs with the same pattern as in uninfected cells. Bar is equivalent to 10 μm.

internal edges of ASF/SF2 ring structures (Fig. 3C, also shown enlarged in Fig. 6B). The accumulation of E2A-72K as discrete spots and rings, containing ssDNA displaced from viral DNA replication, indicates the onset of the viral late phase and demarcates sites of active replication (Pombo et al., 1994; Puvion-Dutilleul and Puvion, 1990a, 1990b, 1992). The CB rosettes form at the periphery of the ssDNA pools and we have shown that they are distinct from the replication foci that also localise to the periphery of the ssDNA domains (Pombo et al., 1994; Aspegren et al., 1998). These data are combined in a schematic representation shown in Fig. 6C. Moreover,

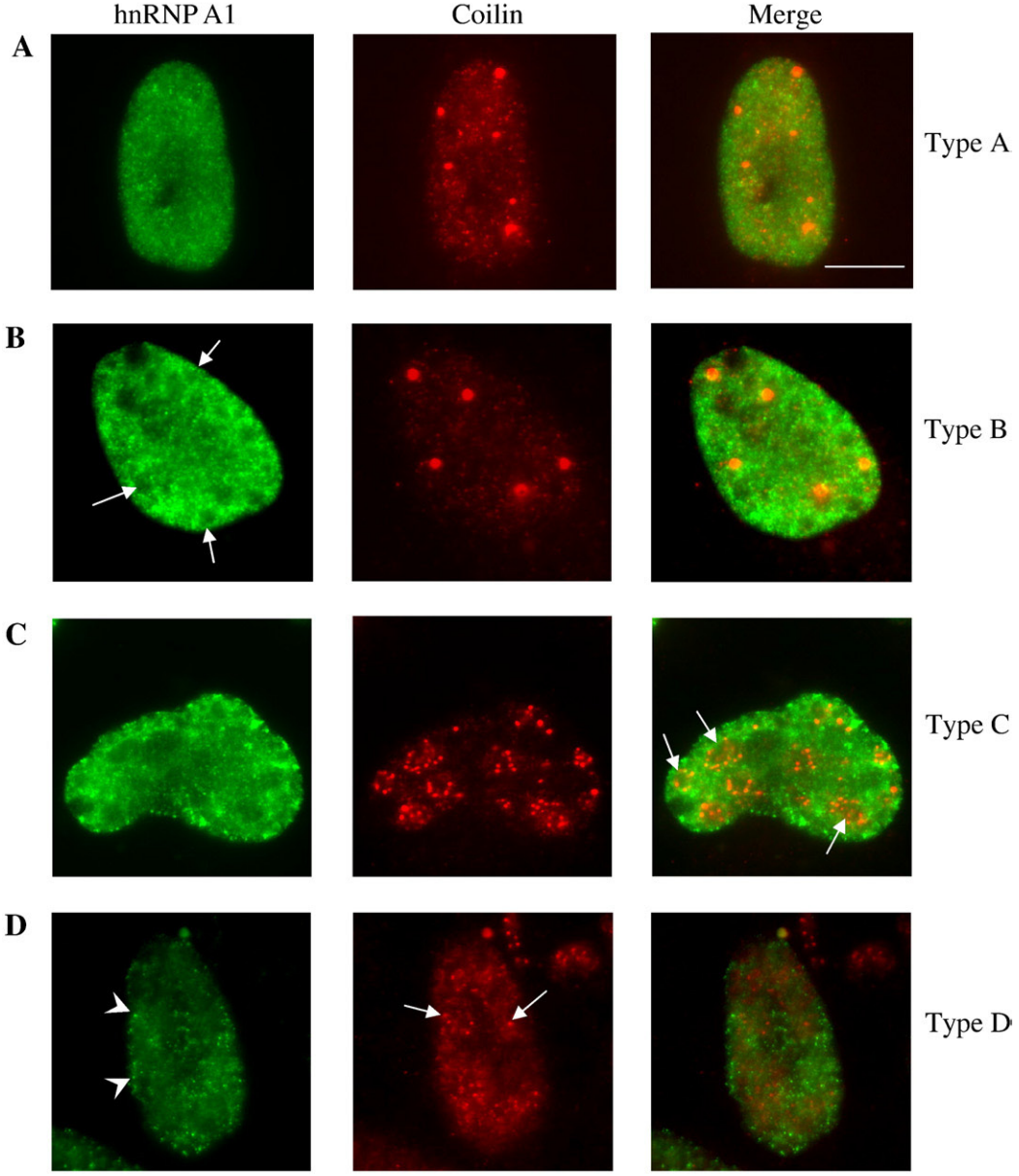

	0	4	8	12	16	20
A	100	100	100	61	62	39
B	0	0	0	29	0	11
C	0	0	0	11	0	0
D	0	0	0	0	38	50

Type	CB pattern	hnRNP A1 pattern
A	Uninfected	Speckles
B	Uninfected	Rings
C	Rosettes	Rings
D	Clusters	Clusters

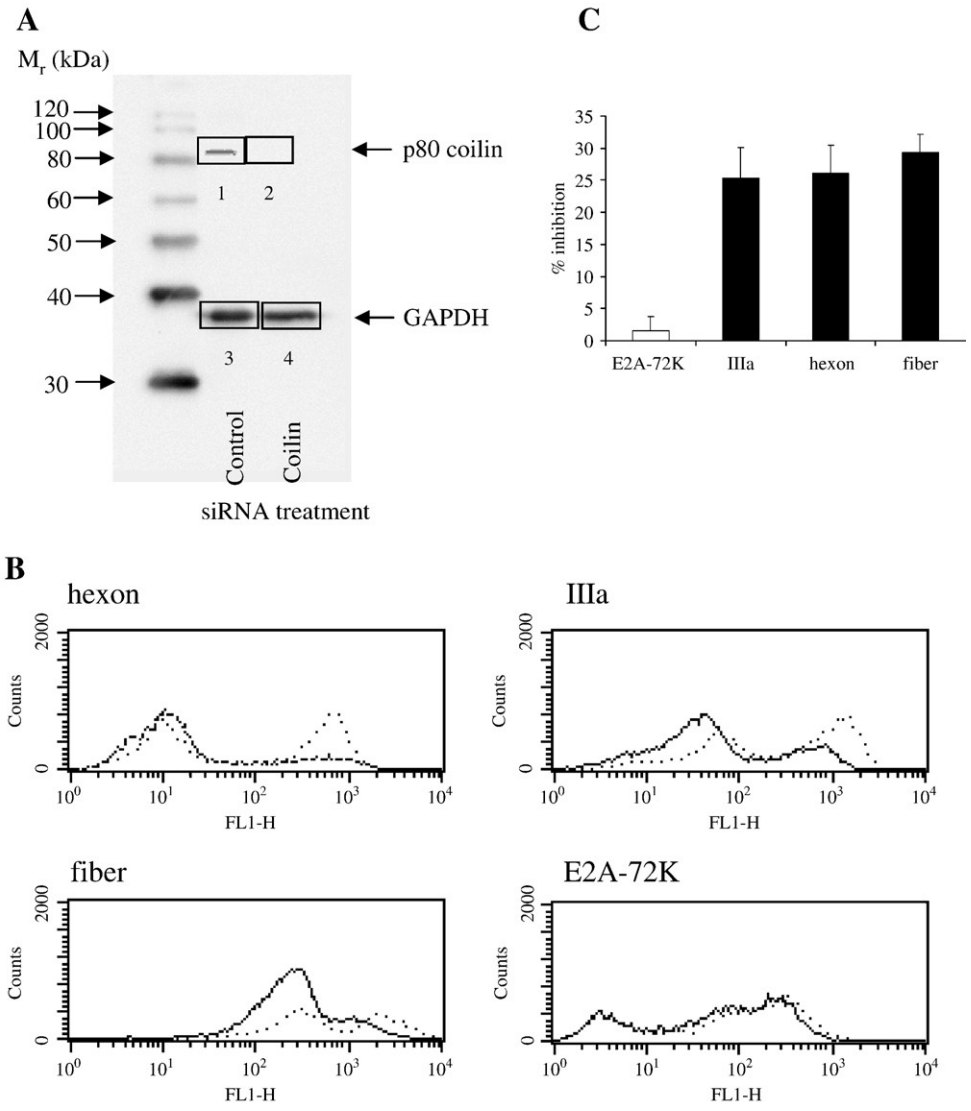

Fig. 5. Coilin knock-down inhibits the expression of alternatively spliced late phase proteins. HeLa cells were transfected with control siRNA or coilin siRNA for 24 h then infected with Ad5 (1000 FFU/cell) prior to a second 24-h treatment with control or coilin siRNA. (A) Western blot of coilin and GAPDH of cells. Cells were analysed for reduction of coilin expression by Western blotting, using mouse anti-coilin (1:500) and mouse anti-GAPDH (1:20,000) antibodies followed by incubation with goat anti-mouse HRP and chemiluminescent detection (lanes 1 and 2, control siRNA- and coilin siRNA-treated, respectively). Densitometric analysis was perfomed to obtain values for the band intensities (in pixel densities): 1: 2.77×10^6, 2: 0.60×10^6, 3: 1.99×10^5 and 4: 1.91×10^5. Band intensity of the sample treated with coilin siRNA was expressed as a percentage of the band intensity of the control sample as follows; (intensity of band from coilin siRNA-treated sample/band intensity of control siRNA-treated sample)$\times$100. Coilin knock-down reduced coilin expresssion by 80% but had no effect on GAPDH levels. (B) Representative fluorescence histograms from flow cytometric analysis of levels of E2A-72K, IIIa, hexon and fiber expression after coilin knock-down. Cells were trypsinised, washed in PBS, fixed in 10% formalin and permeabilised in 0.5% Triton-X100. Cells were incubated with saturating concentrations of anti-IIIa, anti-hexon, anti-fiber or anti-E2A-72K followed by incubation with a secondary antibody conjugated to AlexaFluor488. Validation experiments showed that although the position of the nadir on the FL1H axis varied between samples, it defined the threshold for distinguishing positive from negative cells (see Supplementary Fig. 1). The percentage of positive cells was determined by setting a marker at the nadir between the two peaks of FL1H and performing the calculation (number of positive cells/total number of cells)$\times$100. (C) Results of flow cytometric analysis. Collated data from three independent experiments is shown as a histogram. Bars represent mean inhibition ($\pm$SEM).

we have shown that rosette formation occurs after the onset of viral DNA replication and the formation of ASF/SF2 and hnRNP A1 ring structures but before the induction of L4-33K expression (Fig. 6D). The L4-33K and L4-22K products have homologous N-terminal regions. The possibility that the L4-33K antibody may cross-react with L4-22K cannot be excluded (Gambke and Deppert, 1982; Morris and Leppard, 2009). However, since L4-22K is also not expresssed until the late phase and since transcription does not proceed beyond the L3 polyadenylation site in the early phase (Iwamoto et al., 1986), the use of the anti-L4-33K and anti-coilin antibodies seems to form a valid rationale for the determination of the the timing of CB rosette formation.

Fig. 4. Spatiotemporal changes in the distribution of coilin relative to hnRNP A1. HeLa cells were infected with Ad5 (1000 FFU/cell) and harvested at four-hourly intervals up to 20 hpi. Cells were fixed, permeabilised and stained with rabbit anti-coilin and AlexaFluor594-conjugated goat anti-rabbit secondary antibodies (red) followed by mouse anti-hnRNP A1 and AlexaFluor488-conjugated goat anti-mouse antibodies (green). Immunofluorescence was visualised by microscopy. Images of the staining patterns observed are shown in panels A–D. (A) hnRNP A1 distributed as speckles. (B) hnRNP A1 distributed in ring-like structures (arrows), 12 hpi. (C) CB rosettes localised to the periphery of the hnRNP A1 rings (arrows), 12 hpi. (D) Levels of hnRNP A1 were reduced and localised as discrete spots, (some of which were seen at the nuclear periphery, arrowheads) and CB rosettes appeared to disassemble (arrows) 16 hpi. (E) Time–frequency distribution graph of the different staining patterns and the characteristics of each coilin/hnRNP A1 pattern types. "Uninfected," refers to CBs with the same pattern as in uninfected cells. Bar is equivalent to 10 μm.

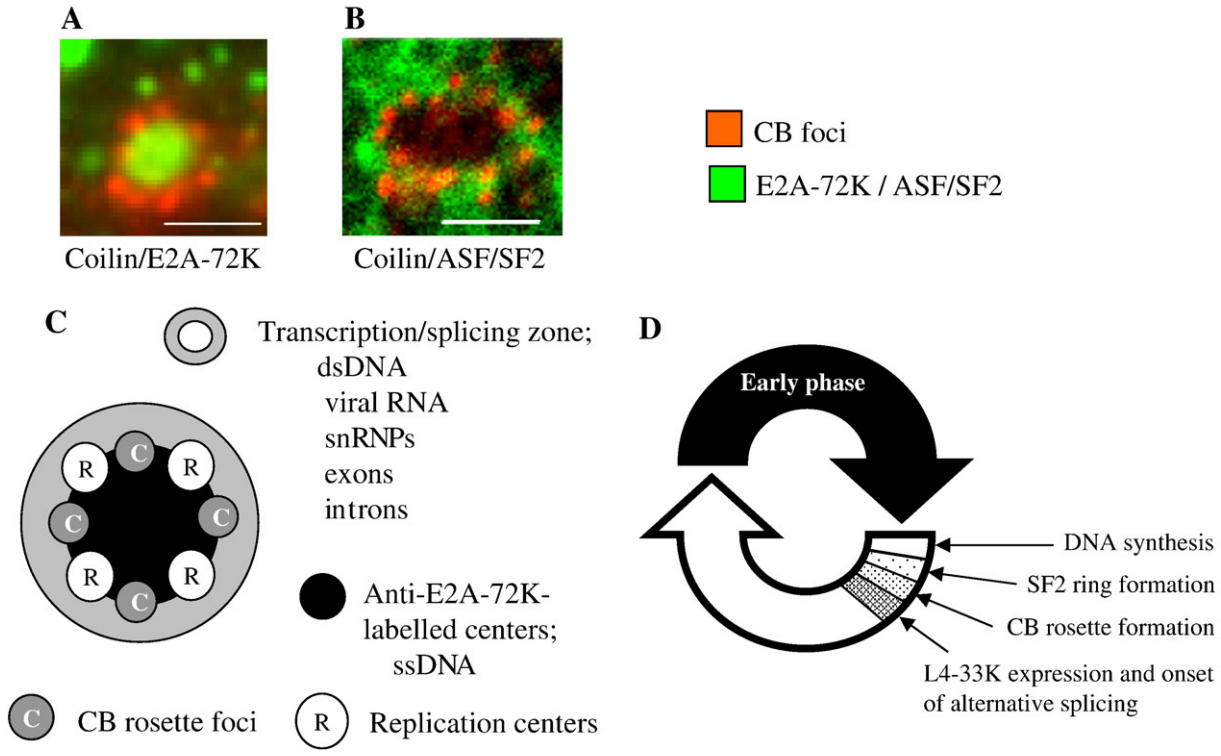

Fig. 6. Organisation and timing of formation of CB rosette structures in the nuclei of adenovirus-infected cells. (A1) Enlarged image of a E2A-72K domain taken from Fig. 2E. CB rosettes (red) localise to the periphery of, and overlap, E2A-72K spots (green). Bar is equivalent to 1 μm. (A2) Enlarged image taken from Fig. 3C. CB rosettes (red) localise to the edges of, and overlap, ASF/SF2 ring structures (green). (B) Schematic representation of the organisation of CB rosettes, replication foci, ssDNA sites and transcription and replication sites in the nucleus of an adenovirus-infected cell in the intermediate phase. (C) Scheme depicting the timing of CB rosette formation within the intermediate phase of the virus life cycle. Early phase (filled black arrow), intermediate phase (graduated shading), late phase (unshaded part of arrow).

ASF/SF2 ring structures form after the onset of DNA synthesis (Aspegren et al., 1998). Since we have shown that the CB rosettes assembled after the formation of ASF/SF2 and hnRNP A1 rings and before the expression of L4-33K, it therefore appears that ASF/SF2 and hnRNP A1 ring structures must also form prior to the expression of L4-33K. The L4-33K product is both necessary and sufficient to enhance alternative splicing of the L1 unit of the MLTU, favoring production of L1-IIIa at the expense of L1-52,55K (Farley et al., 2004; Larsson et al., 1992; Tormanen et al., 2006; Chow et al., 1979; Akusjarvi and Persson, 1981; Nevins and Wilson, 1981). The onset of DNA replication is immediately followed by an intermediate phase characterised by over-expression of L1-IIIa mRNA (Larsson et al., 1992). Our data indicate that the transition to preferential production of L1-IIIa transcripts (as opposed to L1-52,55K transcripts from the L1 region) also occurs after the formation of CB rosettes, since L4-33K over-expression is required to favor L1-IIIa production (Farley et al., 2004) and we have shown that selective over-expression of L4-33K occurs after CB rosette formation. The formation of CB rosettes thus occurs within a defined period, occurring just after the onset of late phase DNA synthesis and prior to the onset of the intermediate phase, more specifically between the formation of ASF/SF2 ring structures and L4-33K over-expression (Fig. 6D).

We determined the fate of the CB rosettes through subsequent phases of the viral life cycle. At the onset of the late phase, interconnecting rings of ASF/SF2 surround E2A-72K sites and are indicative of active MLTU transcription (Puvion-Dutilleul and Puvion, 1992; Aspegren et al., 1998). The ring structures contain spliced exons derived from the tripartite leader sequence of adenovirus major late mRNA transcripts, indicating that at least partial processing of late mRNA precursors is occuring (Aspegren et al., 1998). We show here that hnRNP A1 also forms ring structures analogous to ASF/SF2 ring structures. At an advanced stage of the late phase of infection, coincident with enhanced viral mRNA export, the ASF/SF2 and hnRNP A1 ring structures disappear and are replaced by enlarged speckles (interchromatin granules) that may attach to the nuclear periphery (cluster cells; Aspegren et al., 1998). Our data indicate that CB rosette structures disappear concomitant with the formation of cluster cells (Figs. 3D and 4D). Taken together, our data indicate that CB rosette formation and ASF/SF2 and hnRNP A1 ring formation are largely concurrent, with CB rosettes forming just after ring formation and CB rosette disassembly coinciding with the dissipation of ASF/SF2 and hnRNP A1 rings.

The function of CB rosette formation may therefore be associated with the transcription/splicing function of the ASF/SF2 and hnRNP A1 ring structures and/or L4-33K induction. Coilin knock-down reduced both the formation of infectious virus and the production of late phase proteins by around 30%. The reduction in coilin expression by RNA interference (80%) was not proportionately reflected in the magnitude of the reduction in late phase protein expression. This apparent discrepancy may be explained by a functional redundancy that has been previously demonstrated, since cells in which coilin activity was reduced (by microinjection of anti-coilin antibodies) remained competent to splice adenovirus pre-mRNA (Almeida et al., 1998). Nevertheless, our data clearly demonstrate that coilin knock-down results in a reduction in the yield of infectious virus. We found that coilin knock-down had no detectable impact upon the reorganisation of PML bodies and nucleoli induced by Ad5 infection. This implies that the reduction in late phase proteins resulting from knock-down of coilin does not involve structural changes in PML bodies or nucleoli, however this does not exclude the existence of functional interactions between these nuclear bodies.

In Fig. 6C the localisation of the foci of CB rosettes in relation to viral DNA replication and viral transcription and splicing zones in the nuclei of adenovirus-infected cells during the short intermediate

phase is schematically depicted. The replication foci surround pools of ssDNA displaced from replication of the first strand of viral DNA. The corresponding replicated dsDNAs are displaced outwards from the replication foci and surround the periphery of the ssDNA pools, where they serve as templates for transcription (Pombo et al., 1994). Transcription sites overlap the replication foci but extend further into the nucleoplasm away from E2A-72K domains, forming patterns of inter-connecting rings (Pombo et al., 1994). The transcription zones also contain nascent viral RNA (Pombo et al., 1994; Puvion-Dutilleul and Puvion, 1992), splicing snRNPs (Aspegren and Bridge, 2002), viral introns and exons (Rebelo et al., 1996; Aspegren et al., 1998; Bridge et al., 1996). The transition from the early to the late phase requires viral gene expression from replicated templates (Chalberg and Kelley, 1989). Hence CBs are ideally positioned relative to the replicated viral DNAs (that are used as late phase transcription templates) to influence the production of late phase transcripts. CBs are involved in the assembly of transcriptosomes as well as the maturation, assembly and recycling of snRNPs in spliceosomal holoenzymes. Reorganisation of CBs into rosettes may be a viral adaptation to increase the productivity of transcription and splicing, perhaps via increased surface area and/or efficient delivery and regeneration of mature transcriptosomes and spliceosomes. Future work will define the mechanism underlying these processes and determine the potential of CBs as targets for anti-viral strategies.

Materials and methods

Cell culture and virus infection

HeLa cell monolayer cultures were maintained in growth medium consisting of Dulbecco's modified minimal essential medium (DMEM) supplemented with 10% fetal calf serum (FCS), penicillin (100 U/ml) and streptomycin (100 μg/ml). Ad5 virus was propagated in HeLa cells and purified by CsCl gradient centrifugation as previously described (Tollefson et al., 1999). Virus titers were determined by the fluorescent focus assay amd expressed as fluorescent focus-forming units (FFU), as previously described (Philipson, 1961).

Antibodies

Rabbit polyclonal anti-coilin and mouse monoclonal anti-coilin antibodies were gifts from Angus Lamond, University of Dundee, Scotland and were used at 1:500 dilution. Mouse monoclonal anti-splicing factor 2 (ASF/SF2) clone 103 was obtained from Zymed Laboratories (San Francisco, USA) and used at a dilution of 1:250. Mouse monoclonal anti-hnRNP A1 clone 4B10 was purchased from ImmuQuest (Cleveland, UK) and used at a dilution of 1:1000. Rabbit polyclonal antibodies against Sp100 and fibrillarin were obtained from Chemicon International (Temecula, California, USA) and AbCam (Cambridge, UK) and used at dilutions of 1:5000 and 1:100 respectively. Rabbit polyclonal anti-LI-IIIa and anti-L4-33K (Gambke and Deppert, 1982) were gifts from Goran Akusjarvi (Uppsala University, Sweden) and Wolfgang Deppert (Hamburg University, Germany) respectively and were used at 1:100. Mouse monoclonal anti-hexon (clone 88.1) was a gift from Ian Sharp (Health Protection Agency, Colindale, London) and was used at 1:100. Mouse monoclonal anti-E2A-72K (clone B6–8) was provided by Keith Leppard (Warwick University, UK) and used at 1:20 (Reich et al., 1983). Rabbit polyclonal anti-fiber serum was produced in our laboratory according to previously described procedures (McDonald et al., 1999) and was used at 1:500. AlexaFluor 488-labelled goat anti-rabbit or goat anti-mouse antibodies were used for detection of primary antibody binding by flow cytometry and also for dual immunofluorescence microscopy, where it was used in conjunction with AlexaFluor 598-conjugated goat anti-mouse or goat anti-rabbit secondary antibodies (both from Invitrogen, Paisley, Scotland); both were used at 1:1000. Horseradish peroxidase (HRP)-conjugated goat anti-mouse immunoglobulin was purchased from Sigma (Poole, Dorset, UK). Mouse monoclonal anti-glyceraldehyde-3-phosphate dehydrogenase (anti-GAPDH) antibody (clone 6C5) was purchased from Calbiochem (Merck Chemicals Limited, Nottingham, UK) and used at 1 in 20,000 for Western blotting. Rat monoclonal anti-BrdU antibody (Immunologicals Direct, Clone BU 1/75) used at 1 in 100 and FITC-conjugated goat anti-rat immunoglobulins (Invitrogen, Paisley, Scotland) used at 1:1000 were gifts from Dean Jackson (University of Manchester, UK).

Immunofluorescence microscopy

Sub-confluent HeLa cells grown on sterile glass coverslips were inoculated with CsCl-purified wild type Ad5 at a multiplicity of infection (moi) of 1000 focus forming units (FFU) per cell (where 100 FFU was equivalent to 1 PFU) in serum-free medium for 1 h at 37 °C. The inoculum was removed and replaced by fresh growth medium. When required, cytosine arabinoside (Ara C) was added to the cultures to 25 μg/ml to inhibit viral DNA replication (Gaynor et al., 1982). All immunofluorescence procedures were performed at room temperature. Cells were washed twice with PBS, fixed in 10% formalin (SigmaFix, Sigma, Poole, Dorset, UK) for 5 min and washed twice with PBS. After fixation, cells were permeabilised with 0.5% (v/v) Triton X-100 in PBS for 5 min, washed with PBS and incubated for 45 min at room temperature with mouse monoclonal antibodies to E2A-72K, ASF/SF2 or hnRNP A1, or rabbit polyclonal antibody to L4-33K, diluted in a solution of PBS containing 2 mM sodium azide and 5% normal goat serum as described above. The cells were subsequently washed twice with PBS and incubated with either AlexaFluor488-conjugated goat anti-mouse or goat anti-rabbit secondary antibody diluted in PBS containing 5% normal goat serum and 2 mM sodium azide. The cells were then incubated with either rabbit polyclonal or mouse monoclonal anti-coilin antibody for 30 min, followed by washing and incubation with AlexaFluor594-conjugated goat anti-rabbit or goat anti-mouse antibody for 30 min. Nuclei were stained with 1 μg/ml 4′,6-diamidino-2-phenylindole (DAPI) for 2 min, prior to mounting in VectaShield (Vector Laboratories, Peterborough, UK). Cells were viewed using a Zeiss AxioPlan 2 microscope. Zeiss filter sets 2, 10 and 15 were used for detection of fluorescence emissions from DAPI, AlexaFluor 488 and AlexaFluor 594, respectively. Images were captured and analysed using AxioVision Software (Carl Zeiss MicroImaging GmbH, Göttingen, Germany).

Detection of viral replication foci

HeLa cells grown on sterile glass coverslips were infected with Ad5 as described above. After 24 h, BrdU was added directly to the medium to a final concentration of 25 μM. After 60 min at 37 °C, cells were harvested and washed twice with PBS. All subsequent steps were performed at room temperature. Cells were fixed in 10% formalin for 10 min, washed with PBS and permeabilised for 5 min in PBS containing 0.5% Triton X-100. After a further two washes in PBS, cells were incubated in PBS containing 100 μg/ml DNase II (Roche Diagnostics GmbH, Mannheim, Germany). After 30 min, cells were washed in PBS and incubated with rat anti-BrdU in PBS containing 5% normal goat serum and 2 mM sodium azide for 1 h. Cells were washed in PBS and incubated with FITC-conjugated goat anti-rat antibody for 45 min. Cells were then incubated with rabbit anti-coilin (1:500) followed by goat anti-rabbit AlexaFluor 594 (1:1000) for 45 min each, with an intervening wash in PBS. Coverslips were mounted in VectaShield (Vector Laboratories Ltd, Peterborough, UK) prior to examination by fluorescence microscopy.

RNA interference

Twenty four hours prior to transfection with siRNA, HeLa cells (0.2×10^6) were plated on sterile glass coverslips in wells of a six-well plate in DMEM containing 10% FCS and 2 mM L-glutamine in the

absence of antibiotics. siRNAs were synthesised by Eurogentec Ltd. (Southampton, UK) as PAGE-purified duplexes with double deoxythymidine overhangs at the 3′ ends. The upper strand sequences, in the 5′ to 3′ direction, were ATTTCTCCGAACGTGTCACGT and GAGAGGAGUUGCUGAGAAU for the control and coilin siRNAs respectively. For each sample well, two separate solutions were prepared: the first comprised 3 μl of Lipofectamine 2000 (Invitrogen, Paisley, Scotland) and 250 μl of DMEM and the second, 20 μl of a 20 μM stock of siRNA and 250 μl of DMEM. The two solutions were incubated separately at room temperature for 10 min prior to mixing. The complete transfection mixture was incubated for a further 15 min prior to addition to the cells, which had been previously washed in serum-free DMEM and resuspended in 1.5 ml of serum-free DMEM. In order to obtain maximum coilin knock-down and minimal cell toxicity, the transfection was performed twice, the second siRNA transfection carried out 24 h after the first. In both transfections, after 4 h the transfection medium was removed and replaced with DMEM containing 10% FCS and 2 mM L-Glutamine. The second round of coilin knock-down was immediately preceded by infection with wild type Ad5 as described above. Twenty-four hours after the second transfection, cells were harvested using trypsin for flow cytometric analysis and quantitation of protein expression.

SDS-PAGE and Western blotting

HeLa cells grown in six-well plates were washed with PBS. Cell lysates were prepared by scraping the cells into 100 μl of RIPA buffer (150 mM NaCl, 1% (v/v) Nonidet P40 (BDH, Poole, UK), 0.5% (w/v) sodium deoxycholate, 0.1% (w/v) sodium dodecyl sulfate and 50 mM Tris–HCl, pH 8.0) supplemented with one protease inhibitor cocktail tablet (Roche, Mannheim, Germany) per 50 ml RIPA buffer. Aliquots (5 μl) of 5× sample buffer (250 mM Tris-HCl, pH 6.8, 10% SDS, 5% β-mercaptoethanol, 50% glycerol and 0.05% bromophenol blue) were added to 25 μl samples of cell lysates and boiled at 100 °C for 5 min. Samples were separated by electrophoresis in 12% SDS-PAGE gels using a mini-gel system (Atto, Tokyo, Japan). Proteins were transferred to PVDF membranes using a semi-dry blotting system (Biometra, Goettingen, Germany) at 16 V for 1 h. The membrane was blocked for 1 h in PBS-T (PBS containing 0.1% (v/v) Tween-20) supplemented with 10% (w/v) non-fat dry milk. The membrane was then incubated for 1 h at room temperature in PBS-T containing mouse monoclonal antibodies against coilin and GAPDH. The membrane was then washed with PBS-T prior to incubation for 1 h at room temperature in PBS-T containing HRP-conjugated goat anti-mouse immunoglobulin. Blots were developed using ECL Advanced chemiluminescence detection kit (Amersham, Little Chalfont, UK) and detected using a FujiFilm LAS 3000 luminescent image analyser (FujiFilm Life Science, Stamford, CT). Band intensities were analysed using Aida image analysis software (Raytest GmbH, Straubenhardt, Germany).

Flow cytometry

Cells were detached from coverslips using trypsin and dispensed into microcentrifuge tubes. The cells were washed with PBS, fixed in 10% formalin for 10 min, washed and permeabilised with 0.5% (v/v) Triton X-100 in PBS for 10 min prior to a final wash in PBS. Cells were incubated for 30 min in the presence of an appropriate dilution of primary antibody (see above) against: Ad5 IIIa, hexon, fiber or E2A-72K. Bound primary antibodies were detected using AlexaFluor488-conjugated goat secondary antibodies. Cells were analysed for peak height fluorescence in the FL1 channel using a FACS Calibur flow cytometer (Becton Dickinson UK Ltd., Oxford, UK), with a 530/30 bandpass dichroic mirror.

Fluorescence intensity histograms were analysed using CellQuest Pro software (Becton Dickinson UK Ltd., Oxford, UK). Quantitation of L1-IIIa, L3-hexon and L5-fiber expression in infected cells was determined as previously described (Bottley et al., 2007). The procedure was validated to ensure that the measurement of fluorescence emission by flow cytometry was proportional to the level of viral antigen; E2A-72K, hexon, IIIa and fiber. Antibody staining produced bimodal peaks, where the nadir distinguished the negative from the positive cells. Fluorescence intensity was at least 10-fold greater for positive compared to negative cells (Supplementary Figure 1). A marker was set at the nadir and the number of cells that were positive for the antigen in question was calculated as follows; (number of positive cells / total number of cells) × 100.

Assay of virus yield by second-round re-infection

Cells infected with Ad5 following treatment with coilin or control siRNA were detached using trypsin and washed with PBS. For assay of virus yield by second round infection (reinfection), the pellet was resuspended in 100 μl of PBS and an equivalent volume of sterile water was added. The cells were left on ice for 30 min prior to freezing at –20 °C. The lysed cells were thawed and sonicated in a bath-type sonicator for two minutes. Sonicated cell extracts were resuspended in two ml of DMEM and then added to cells which had been plated at 0.2×10^6 cells per well of a 6-well plate one day prior to infection. Cells were incubated in the presence of the virus-containing lysate for 20 h and hexon expression was determined by flow cytometry as described above.

Acknowledgments

This work was supported by Yorkshire Cancer Research and the Biotechnology and Biological Sciences Research Council (BBSRC). We thank Dean Jackson and Apolinar Maya-Mendoza for help with analysis of replication sites and Natalie Fox, Joan Jarvis and John Holt for technical assistance and advice.

Appendix A. Supplementary data

Supplementary data associated with this article can be found, in the online version, at doi:10.1016/j.virol.2010.01.013.

References

Akusjarvi, G., Persson, H., 1981. Controls of RNA splicing and termination in the major late adenovirus transcription unit. Nature 292, 420–426.
Alliegro, M.C., Alliegro, M.A., 1998. Protein heterogeneity in the coiled body compartment. Exp. Cell Res. 239, 60–68.
Almeida, F., Saffrich, R., Ansorge, W., Carmo-Fonseca, M., 1998. Microinjection of anti-coilin antibodies affects the structure of coiled bodies. J. Cell Biol. 142, 899–912.
Alzhanova-Ericsson, A.T., Sun, X., Visa, N., Kiseleva, E., Wurtz, T., Daneholt, B., 1996. A protein of the SR family of splicing factors binds extensively to exonic Balbiani ring pre-mRNA and accompanies the RNA from the gene to the nuclear pore. Genes Dev. 10, 2881–2893.
Andrade, L.E., Tan, E.M., Chan, E.K., 1993. Immunocytochemical analysis of the coiled body in the cell cycle and during cell proliferation. Proc. Natl Acad. Sci. U.S.A. 90, 1947–1951.
Aspegren, A., Bridge, E., 2002. Release of snRNP and RNA from transcription sites in adenovirus-infected cells. Exp. Cell Res. 276, 273–283.
Aspegren, A., Rabino, C., Bridge, E., 1998. Organization of splicing factors in adenovirus-infected cells reflects changes in gene expression during the early to late phase transition. Exp. Cell Res. 245, 203–213.
Bai, Y., Lee, D., Yu, T., Chasin, L.A., 1999. Control of 3′ splice site choice in vivo by ASF/SF2 and hnRNP A1. Nucleic Acids Res. 27, 1126–1134.
Bauren, G., Wieslander, L., 1994. Splicing of Balbiani ring 1 gene pre-mRNA occurs simultaneously with transcription. Cell 76, 183–192.
Bentley, D., 1999. Coupling RNA polymerase II transcription with pre-mRNA processing. Curr. Opin. Cell Biol. 347-351, 11 1999.
Bettinger, B.T., Gilbert, D.M., Amberg, D.C., 2004. Actin up in the nucleus. Nat. Rev. Mol. Cell Biol. 5, 410–415.
Beyer, A.L., Osheim, Y.N., 1988. Splice site selection, rate of splicing, and alternative splicing on nascent transcripts. Genes Dev. 2, 754–765.
Blair, G.E., James, N.J., 2005. DNA viruses and the nucleus. In: Hiscox, J.A. (Ed.), Viruses and the Nucleus. John Wiley & Sons, Ltd, pp. 69–87.
Bottley, G., Holt, J.R., James, N.J., Blair, G.E., 2007. Flow cytometric detection of adenoviruses and intracellular adenovirus proteins. Methods Mol. Med. 130, 205–213.
Bridge, E., Pettersson, U., 1996. Nuclear organization of adenovirus RNA biogenesis. Exp. Cell Res. 229, 233–239.

Bridge, E., Xia, D.X., Carmo-Fonseca, M., Cardinali, B., Lamond, A.I., Petterssen, U., 1995. Dynamic organisation of splicing factors in adenovirus-infected cells. J. Virol. 69, 281–290.
Bridge, E., Riedel, K., Johansson, B., Pettersson, U., 1996. Spliced exons of adenovirus late RNAs colocalize with snRNP in a specific nuclear domain. J. Cell Biol. 135, 303–314.
Cajal, S. Ramón y., 1903. Un sencillo metodo de coloracion seletiva del reticulo protoplasmatico y sus efectos en los diversos organos nerviosos de vertebrados e invertebrados. Trab. Lab. Invest. Biol. (Madrid) 2, 129–221.
Carmo-Fonseca, M., Ferreira, J., Lamond, A.I., 1993. Assembly of snRNP-containing coiled bodies is regulated in interphase and mitosis—evidence that the coiled body is a kinetic nuclear structure. J. Cell Biol. 120, 841–852.
Chalberg, M.D., Kelley, T.J., 1989. Animal virus DNA replication. Ann. Rev. Biochem. 58, 671–717.
Chow, L.T., Broker, T.R., Lewis, J.B., 1979. Complex splicing patterns of RNAs from the early regions of adenovirus 2. J. Mol. Biol. 134, 265–303.
Cioce, M., Lamond, A.I.., 2005. Cajal bodies: a long history of discovery. Ann. Rev. Cell Dev. Biol. 21, 105–131.
Cmarko, D., Verschure, P.J., Martin, T.E., Dahmus, M.E., Krause, S., Fu, X.D., van Driel, R., Fakan, S., 1999. Ultrastructural analysis of transcription and splicing in the cell nucleus after bromo-UTP microinjection. Mol. Biol. Cell 10, 211–223.
Dundr, M., Hebert, M.D., Karpova, T.S., Stanek, D., Xu, H., Shpargel, K.B., Meier, U.T., Neugebauer, K.M., Matera, A.G., Misteli, T., 2004. In vivo kinetics of Cajal body components. J. Cell Biol. 164, 831–842.
Farley, D.C., Brown, J.L., Leppard, K.N., 2004. Activation of the early-late switch in adenovirus type 5 major late transcription unit expression by L4 gene products. J. Virol. 78, 1782–1791.
Fernandez, R., Pena, E., Navascues, J., Casafont, I., Lafarga, M., Berciano, M.T., 2002. cAMP-dependent reorganization of the Cajal bodies and splicing machinery in cultured Schwann cells. Glia 40, 378–388.
Gall, J.G., 2000. Cajal bodies: the first 100 years. Ann. Rev. Cell Dev. Biol. 16, 273–300.
Gama-Carvalho, M., Condado, I., Carmo-Fonseca, M., 2003. Regulation of adenovirus alternative RNA splicing correlates with a reorganization of splicing factors in the nucleus. Exp. Cell Res. 289, 77–85.
Gambke, C., Deppert, W., 1982. Late non-structural 100,000 and 33,000-Dalton proteins of adenovirus type 2. I. Subcellular localisation during the course of infection. J. Virol. 40, 585–593.
Gaynor, R.B., Tsukamoto, A., Montell, C., Berk, A.J., 1982. Enhanced expression of adenovirus transforming proteins. J. Virol. 44, 276–285.
Gedge, L.J., Morrison, E.E., Blair, G.E., Walker, J.H., 2005. Nuclear actin is partially associated with Cajal bodies in human cells in culture and relocates to the nuclear periphery after infection of cells by adenovirus 5. Exp. Cell Res. 303, 229–239.
Grande, M.A., van der Kraan, I., van Steensel, B., Schul, W., de The, H., van der Voort, H.T., de Jong, L., van Driel, R., 1996. PML-containing nuclear bodies: their spatial distribution in realtion to other nuclear components. J. Cell. Biochem. 63, 280–291.
Green, M., Daesch, G.E., 1961. Biochemical studies on adenovirus multiplication I. Kinetics of nucleic acid and protein synthesis in suspension cultures. Virology 13, 169–176.
Herbert, M.D., Szymczyk, P.W., Shpargel, K.B., Matera, A.G., 2001. Coilin forms the bridge between Cajal bodies and SMN, the spinal muscular atrophy protein. Genes Dev. 15, 2720–2729.
Iwamoto, S., Eggerding, F., Falck-Pederson, E., Darnell, J.E., 1986. Transcription unit mapping in adenovirus: regions of termination. J. Virol. 59, 112–119.
Jordan, P., Cunha, C., Carmo-Fonseca, M., 1997. The cdk7-cyclin H-MAT1 complex associated with TFIIH is localized in coiled bodies. Mol. Biol. Cell 8, 1207–1217.
Larsson, S., Svensson, C., Akusjarvi, G., 1992. Control of adenovirus major late gene expression at multiple levels. J. Mol. Biol. 225, 287–298.
McDonald, D., Stockwin, L., Matzow, T., Blair-Zajdel, M.E., Blair, G.E., 1999. Coxsackie and adenovirus receptor (CAR)-dependent and major histocompatibility complex (MHC) class I-independent uptake of recombinant adenoviruses into human tumour cells. Gene Ther. 6, 1512–1519.
Morris, S.J., Leppard, K.N., 2009. Adenovirus serotype 5 L4-22K and L4-33K proteins have distinct functions in regulating late gene expression. J. Virol. 83, 3049–3058.
Müller, S., Dejean, A., 1999. Viral immediate-early proteins abrogate the modification by SUMO-1 of PML and Sp100 proteins, correlating with nuclear body disruption. J. Virol. 73, 5137–5143.
Neugebauer, K.M., Roth, M.B., 1997. Distribution of pre-mRNA splicing factors at sites of RNA polymerase II transcription. Genes Dev. 11, 1148–1159.
Nevins, J.R., 1983. The pathway of eukaryotic mRNA formation. Ann. Rev. Biochem. 52, 441–466.
Nevins, J.R., Darnell, J.E., 1978. Steps in the processing of Ad2 mRNA: poly(A)+ nuclear sequences are conserved and poly(A) addition precedes splicing. Cell 15, 1477–1493.
Nevins, J.R., Wilson, M.C., 1981. Regulation of adenovirus 2 gene expression at the level of transcriptional termination and RNA processing. Nature 290, 113–118.
Philipson, L., 1961. Adenovirus assay by the fluorescent cell-counting procedure. Virology 15, 263–268.
Platani, M., Goldberg, I., Swedlow, J.R., Lamond, A.I., 2000. In vivo analysis of Cajal body movement, separation, and joining in live human cells. J. Cell Biol. 151, 1561–1574.
Pombo, A., Ferreira, J., Bridge, E., Carmo-Fonseca, M., 1994. Adenovirus replication and transcription sites are spatially separated in the nucleus of infected cells. EMBO J. 13, 5075–5085.
Puvion-Dutilleul, F., Puvion, E., 1990a. Analysis by in situ hybridization and autoradiography of sites of replication and storage of single- and double-stranded adenovirus type 5 DNA in lytically infected HeLa cells. J. Struct. Biol. 103, 280–289.
Puvion-Dutilleul, F., Puvion, E., 1990b. Replicating single-stranded adenovirus type 5 DNA molecules accumulate within well-delimited intranuclear areas of lytically infected HeLa cells. Eur. J. Cell Biol. 52, 379–388.
Puvion-Dutilleul, F., Puvion, E., 1992. Distribution of viral RNA molecules during the adenovirus type 5 infectious cycle in HeLa cells. J. Struct. Biol. 108, 209–220.
Puvion-Dutilleul, F., Christensen, M.E., 1993. Alterations of fibrillarin distribution and nucleolar ultrastructure induced by adenovirus infection. Eur. J. Cell Biol. 61, 168–176.
Raska, I., 1995. Nuclear ultrastructures associated with the RNA synthesis and processing. J. Cell. Biochem. 59, 11–26.
Rebelo, L., Almeida, F., Ramos, C., Bohmann, K., Lamond, A.I., Carmo-Fonseca, M., 1996. The dynamics of coiled bodies in the nucleus of adenovirus-infected cells. Mol. Biol. Cell 7, 1137–1151.
Reddy, R., Busch, H., 1998. Small nuclear RNAs: RNA sequences, structure and modifications. In: Birnstiel, M.L. (Ed.), Structure and Function of Major and Minor Small Nuclear Ribonucleoprotein Particles. Springer, Berlin, Germany, pp. 1–37.
Reich, N.C., Sarnow, P., Duprey, E., Levine, A.J., 1983. Monoclonal antibodies which recognize native and denatured forms of the adenovirus DNA-binding protein. Virology 128, 480–484.
Rodrigues, S.H., Silva, N.P., Delicio, L.R., Granato, C., Andrade, L.E., 1996. The behavior of the coiled body in cells infected with adenovirus in vitro. Mol. Biol. Rep. 23, 183–189.
Schul, W., Groenhout, B., Koberna, K., Takagaki, Y., Jenny, A., Manders, E.M., Raska, I., van Driel, R., de Jong, L., 1996. The RNA 3′ cleavage factors CstF 64 kDa and CPSF 100 kDa are concentrated in nuclear domains closely associated with coiled bodies and newly synthesized RNA. EMBO J. 15, 2883–2892.
Shaw, A.R., Ziff, E.B., 1980. Transcripts from the adenovirus-2 major late promoter yield a single early family of 3′ co-terminal mRNAs and five late families. Cell 22, 905–916.
Sleeman, J.E., Lamond, A.I., 1999. Nuclear organization of pre-mRNA splicing factors. Curr. Opin. Cell Biol. 11, 372–377.
Sleeman, J.E., Ajuh, P., Lamond, A.I., 2001. snRNP protein expression enhances the formation of Cajal bodies containing p80-coilin and SMN. J. Cell. Sci. 114, 4407–4419.
Sleeman, J.E., Trinkle-Mulcahy, L., Prescott, A.R., Ogg, S.C., Lamond, A.I., 2003. Cajal body proteins SMN and Coilin show differential dynamic behaviour in vivo. J. Cell. Sci. 116, 2039–2050.
Smith, C.W., Valcarcel, J., 2000. Alternative pre-mRNA splicing: the logic of combinatorial control. Trends Biochem. Sci. 25, 381–388.
Smith, K.P., Carter, K.C., Johnson, C.V., Lawrence, J.B., 1995. U2 and U1 snRNA gene loci associate with coiled bodies. J. Cell. Biochem. 59, 473–485.
Tollefson, A.E., Hermiston, T.W., Wold, W.S.M., 1999. Preparation and titration of CsCl-banded Adenovirus stock. In: Wold, W.S.M. (Ed.), Adenovirus Methods and Protocols. Humana Press, Totowa, New Jersey.
Tormanen, H., Backstrom, E., Carlsson, A., Akusjarvi, G., 2006. L4-33K, an adenovirus-encoded alternative RNA splicing factor. J. Biol. Chem. 281, 36510–36517.
Tucker, K.E., Berciano, M.T., Jacobs, E.Y., LePage, D.F., Shpargel, K.B., Rossire, J.J., Chan, E.K., Lafarga, M., Conlon, R.A., Matera, A.G., 2001. Residual Cajal bodies in coilin knockout mice fail to recruit Sm snRNPs and SMA the spinal muscular atrophy gene product 154: 293-307.
Visa, N., Alzhanova-Ericsson, A.T., Sun, X., Kiseleva, E., Bjorkroth, B., Wurtz, T., Daneholt, B., 1996a. A pre-mRNA-binding protein accompanies the RNA from the gene through the nuclear pores and into polysomes. Cell 84, 253–264.
Visa, N., Izaurralde, E., Ferreira, J., Daneholt, B., Mattaj, I.W., 1996b. A nuclear cap-binding complex binds Balbiani ring pre-mRNA cotranscriptionally and accompanies the ribonucleoprotein particle during nuclear export. J. Cell Biol. 133, 5–14.
Weitzman, M.D., Ornelles, D.A, 2005. Inactivating intracellular antiviral responses during adenovirus infection. Oncogene 24, 7686–7696.
Xie, S.Q., Pombo, A., 2006. Distribution of different phosphorylated forms of RNA polymerase II in relation to Cajal and PML bodies in human cells: an ultrastructural study. Histochem. Cell Biol. 125, 21–31.
Zeng, C., Kim, E., Warren, S.L., Berget, S.M., 1997. Dynamic relocation of transcription and splicing factors dependent upon transcriptional activity. EMBO J. 16, 1401–1412.